



## Full Length Article

## Information fusion in wireless sensor networks with source correlation

Gianluigi Ferrari<sup>a</sup>, Marco Martalò<sup>a,\*</sup>, Andrea Abrardo<sup>b</sup><sup>a</sup> *Wireless Ad-hoc and Sensor Networks (WASN) Laboratory, Department of Information Engineering, University of Parma, Italy*<sup>b</sup> *Department of Information Engineering, University of Siena, Italy*

## ARTICLE INFO

## Article history:

Received 23 March 2010

Received in revised form 17 January 2012

Accepted 29 September 2012

Available online 11 October 2012

## Keywords:

Central estimating officer (CEO) problem

Information fusion

Wireless sensor networks

Source correlation

Joint channel decoding (JCD)

## ABSTRACT

In this paper, we consider a central estimating officer (CEO) scenario, where sensors observe a noisy version of a binary sequence generated by a single source (the “phenomenon”) and the access point (AP)’s goal is to estimate, by properly fusing the received data, this sequence. Due to this system model, the data sent by the sensors are correlated and, therefore, it is possible to exploit a proper a priori information in the localized fusion operation performed at the AP. In the presence of channel coding at the sensors and block faded communication links, we first derive the optimum maximum a priori probability (MAP) joint decoding and fusion rule, showing its computational unfeasibility. We then derive two suboptimal decoding/fusion strategies. In the first case, the fusion rule exploits the source correlation and receives, at its input, the soft-output values generated by a joint channel decoder (JCD). Two possible iterative JCD algorithms are proposed: one with “circular” iterations between the component decoders (associated with the sources) and one with “parallel” iterations between the component decoders. For each algorithm, two information combining strategies are considered. In the second case, a separate channel decoding (SCD) scheme is considered and the correlation is exploited only during the fusion operation. Our results show that the scheme with SCD followed by fusion basically leads to the same probability of decision error of the scheme with JCD and fusion with, however, a much lower computational complexity, thus making it suitable to resource-constrained scenarios.

© 2012 Elsevier B.V. All rights reserved.

## 1. Introduction

Wireless multiple access schemes, where correlated signals, observed at different nodes, need to be transferred to one or more collectors, model several communication scenarios. For example, these schemes apply to wireless sensor networks, where a set of nodes collect and transmit correlated data to a common sink in an energy-efficient way [1]. In the case of a single collector node (the access point, AP), the design of efficient transmission mechanisms is often referred to as reach-back channel problem [2–4]. Assuming orthogonal additive white Gaussian noise (AWGN) channels between the nodes and the collector, the separation between source and channel coding is known to be optimal [4]. This means that the theoretical limit can be achieved by, first, compressing each source up to its Slepian–Wolf (SW) limit and, then, utilizing independent capacity-achieving channel codes (one per source) [5]. In an attempt to exploit such correlation, many works have recently focused on the design of distributed source coding schemes that approach the SW fundamental limit on the achievable compression rate [6,7].

An alternative solution to distributed source coding is given by joint source channel coding (JSCC) schemes, where the correlated sources are not source encoded but only channel encoded and the source correlation is exploited at the decoder, which jointly recovers the information signals of all sources. For this reason, this approach is also referred to as joint channel decoding (JCD) [8–10]. In this scenario, the presence of block-faded channels may dramatically degrade the performance, unless some countermeasures are taken at the transmitters to protect highly-faded links.

In this paper, we analyze an instance of the so-called central estimating officer (CEO) problem [11]. More precisely, the information sequences at the input of the sensors correspond to noisy observations of the sequence output by a single binary source. The AP’s goal, upon reception of proper information from the sensors, is to estimate the source sequence. While we first derive the optimal maximum a posteriori (MAP) estimation strategy, we then propose suboptimal (but computationally feasible) estimation strategies. A first suboptimal strategy makes use of JCD, followed by a proper fusion of the soft-output values generated by the JCD algorithm. We directly compare two possible JCD algorithms: with circular and parallel iterations (with soft information exchange) between the component decoders, respectively. According to the fusion strategy, source correlation is exploited in both JCD and fusion operations. Two possible strategies to combine the

\* Corresponding author.

E-mail addresses: [gianluigi.ferrari@unipr.it](mailto:gianluigi.ferrari@unipr.it) (G. Ferrari), [marco.martalò@unipr.it](mailto:marco.martalò@unipr.it) (M. Martalò), [abrardo@dii.unisi.it](mailto:abrardo@dii.unisi.it) (A. Abrardo).

information sequences output by the component decoders are considered. In order to reduce the complexity of the decoding operation, we propose a second scheme where the source correlation is not exploited by the decoders, which decode independently of each other, but only in the fusion operation. We denote this scheme as separate channel decoding (SCD) followed by fusion. Our results show that the probability of decision error, after fusion, slightly depends on the particular channel decoding strategy, either joint or separate. This suggests, in more general terms, that the presence of information fusion may have a relevant impact on the channel coding/decoding strategy. For instance, in the considered CEO scenario the presence of fusion makes the use of JCD irrelevant.

This paper is structured as follows. In Section 2, preliminaries on the system model are provided. In Section 3, optimal and sub-optimal decoding and fusion strategies are derived for the scenario of interest. Numerical results are presented and discussed in Section 4, whereas Section 5 concludes the paper.

## 2. System model

### 2.1. Communication scheme

Consider  $n$  spatially distributed nodes which detect (i.e., receive at their inputs) binary information sequences  $\mathbf{x}^{(k)} = [x_0^{(k)}, \dots, x_{L-1}^{(k)}]$ , where  $k = 1, \dots, n$  and  $L$  is the signals' length (the same for all sensors).<sup>1</sup> The following simple additive correlation model is considered:

$$x_i^{(k)} = b_i \oplus z_i^{(k)} \quad i = 0, \dots, L-1 \quad k = 1, \dots, n$$

where  $\{b_i\}$  are independent and identically distributed (i.i.d.) binary random variables and  $\{z_i^{(k)}\}$  are i.i.d. binary random variables with probability  $\rho$  to be 0 (and  $1 - \rho$  to be 1). In particular, we assume that  $P(b_i = 1) \triangleq p_1$  and  $P(b_i = 0) \triangleq p_0 = 1 - p_1$ , regardless of the value of  $i$ . Obviously, if  $\rho = 0.5$  there is no correlation between the binary information signals  $\{\mathbf{x}^{(k)}\}_{k=1}^n$ , whereas if  $\rho = 1$  the information signals are identical. The random variable  $b_i$  can be interpreted as the status (common to all sources) of a physical phenomenon under observation.

A possible scenario where our model applies is in the presence of  $n$  cameras independently observing the same scene, e.g., a body, from different perspectives. For example, it could be of interest to detect sudden and/or periodic body movements. Following the approach in [12], each camera could extract an average luminosity signal representative of the movements. Obviously, the signals extracted by different cameras would be highly correlated. In this case, transmitting the cameras' data to a common sink and exploiting the residual correlation may improve the performance of an overall decision process. The binary correlation model is also meaningful in wireless sensor networking scenarios where it is of interest to detect if the phenomenon under observation (e.g., temperature, humidity, pressure) overcomes a critical threshold. In Section 4, we will investigate the proposed system performance using "synthetic" data. The application of our algorithms to realistic scenarios, e.g., distributed video processing, goes beyond the scope of this paper and will be subject of future investigation.

According to the chosen correlation model, the a priori joint probability mass function (PMF) of the information signals at the inputs of the  $n$  sensors at the  $i$ th epoch ( $i \in \{0, \dots, L-1\}$ ) can be computed. After a few manipulations, one can show that [13]

$$\begin{aligned} p(\mathbf{x}_i) &= p(\mathbf{x}_i | b_i = 0) p(b_i = 0) + p(\mathbf{x}_i | b_i = 1) p(b_i = 1) \\ &= p_0 \rho^{n_b} (1 - \rho)^{n - n_b} + p_1 (1 - \rho)^{n_b} \rho^{n - n_b} \quad i = 0, \dots, L-1 \end{aligned} \quad (1)$$

where  $\mathbf{x}_i = (x_i^{(1)}, \dots, x_i^{(n)})$  and  $n_b = n_b(\mathbf{x}_i)$  is the number of zeros in  $\mathbf{x}_i$ .

In Fig. 1, the overall model for the CEO scenario of interest is shown. The goal of the AP is that of recovering the information signal  $\mathbf{b} = \{b_i\}_{i=0}^{L-1}$  with the lowest possible probability of error.  $\mathbf{x}^{(k)}$  is the noisy version of  $\mathbf{b}$  observed at the  $k$ th sensor. At this point, the sensor channel encodes the information sequence at its input. Referring to the equivalent low-pass signal representation, we denote as  $\mathbf{s}^{(k)}$  the complex samples transmitted by the  $k$ th sensor and as  $N$  the length of  $\mathbf{s}^{(k)}$ . In the remainder of this work, we will assume the same transmitting rate  $r = L/N$  at all sensors: however, the proposed approach is general and can be applied also to scenarios where the transmitting rate varies from sensor to sensor.

By  $\alpha^{(k)} = [\alpha_0^{(k)}, \dots, \alpha_{N-1}^{(k)}]$  we denote the complex gain vector over the  $k$ th link, which encompasses both path loss and fading, and by  $\eta^{(k)} = [\eta_0^{(k)}, \dots, \eta_{N-1}^{(k)}]$  a complex AWGN vector with variance  $\sigma^2 = N_0/2$ . We assume a block fading model for the communication links between the sensors and the AP: more precisely, the fading coefficient of each link is *constant* for the entire duration of a single packet transmission, i.e.,  $\alpha_i^{(k)} = \alpha^{(k)}$  for  $i = 0, \dots, N-1$ . The fading coefficients are assumed to be independent from link to link and, on a single link, between consecutive packet transmissions.<sup>2</sup>

Their amplitudes  $\{|\alpha^{(k)}|\}_{k=1}^n$  are assumed to be Rayleigh distributed with  $\mathbb{E}[|\alpha^{(k)}|^2] = 1$ . The information sequence at each sensor is channel encoded and we denote as  $\mathbf{v}^{(k)} = [v_0^{(k)}, \dots, v_{N-1}^{(k)}]$  the binary (not modulated) codeword ( $v_i^{(k)} \in \{0, 1\}$ ) generated at the  $k$ th node. For simplicity, we assume that binary phase shift keying (BPSK) is the modulation format, i.e.,  $s_i^{(k)} = y_i^{(k)} \sqrt{E_c^{(k)}}$ , where  $y_i^{(k)} = 2v_i^{(k)} - 1 = \pm 1$  and  $E_c^{(k)}$  is the energy per coded bit transmitted by the  $k$ th node. Indicating by  $P_t^{(k)}$  the transmit power at the  $k$ th node, it holds that  $E_c^{(k)} = P_t^{(k)} T_{\text{bit}}$ , where  $T_{\text{bit}}$  is the bit duration. Since we are considering a block fading model, we assume that the link gains can be perfectly estimated at the AP (e.g., using a short preamble with pilot symbols).

We consider a system with orthogonal links. This is meaningful for wireless sensor networking scenarios where reservation-based (or polling) medium access control (MAC) protocols are chosen. The use of these protocols allows to represent the multiple access channel as a set of parallel orthogonal channels [4].

Under the above assumptions, after matched filtering and carrier-phase estimation, the real observable at the AP, relative to a transmitted sample, can be expressed as

$$r_i^{(k)} = |\alpha^{(k)}| \sqrt{E_c^{(k)}} y_i^{(k)} + \eta_i^{(k)} \quad i = 0, \dots, N-1 \quad k = 1, \dots, n \quad (2)$$

where  $\eta_i^{(k)}$  is an AWGN variable with zero mean and variance  $N_0/2$ . The channel signal-to-noise ratio (SNR) can be defined as

$$\gamma_b = \frac{E_b}{N_0} = \frac{E_c}{rN_0}$$

where we have omitted the dependence on the  $k$ th link, since all communications are supposed to have the same statistical properties.

<sup>1</sup> In Appendix B, a table with a list of mathematical symbols used throughout the paper is provided.

<sup>2</sup> For the sake of notational simplicity, the derivation is carried out considering a single packet transmission act, i.e., we do not use any index to indicate the specific packet.

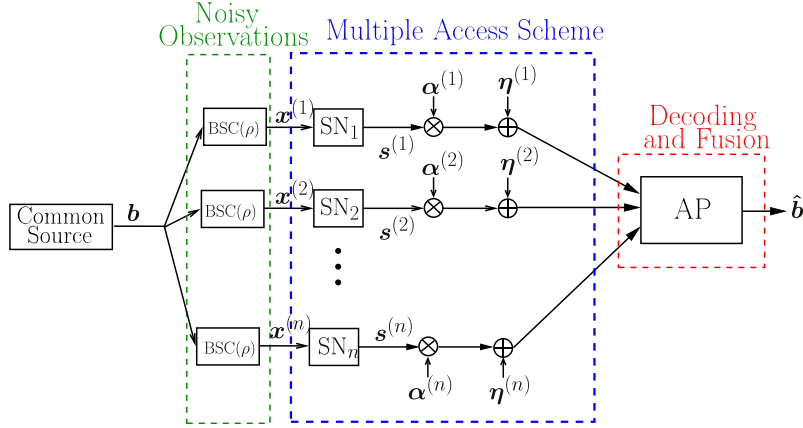


Fig. 1. CEO scenario: multiple access scheme followed by the AP with decoding and fusion.

### 3. Decoding and fusion strategies

#### 3.1. Optimal MAP joint decoding and fusion strategy

In order to estimate the  $i$ th bit emitted by the source, i.e.,  $b_i$  ( $i = 0, \dots, L-1$ ), we consider the following MAP rule:

$$\hat{b}_i \triangleq \arg \max_{b_i=0,1} P(b_i | \mathcal{L}_{\text{ch}}^{(1)}, \dots, \mathcal{L}_{\text{ch}}^{(n)}) \quad (3)$$

where  $\mathcal{L}_{\text{ch}}^{(1)}, \dots, \mathcal{L}_{\text{ch}}^{(n)}$  are the vectors of channel log-likelihood ratios (LLRs) (one for each source) defined as follows<sup>3</sup>:

$$\mathcal{L}_{i,\text{ch}}^{(k)} = \ln \frac{p(r_i^{(k)} | y_i^{(k)} = 1, \alpha_i^{(k)})}{p(r_i^{(k)} | y_i^{(k)} = -1, \alpha_i^{(k)})} = \frac{2r_i^{(k)} \sqrt{E_c^{(k)}} |\alpha_i^{(k)}|}{\sigma^2} \quad (4)$$

$k = 1, \dots, n.$

Using the Bayes' theorem, one obtains:

$$\hat{b}_i = \arg \max_{b_i=0,1} p(\mathcal{L}_{\text{ch}}^{(1)}, \dots, \mathcal{L}_{\text{ch}}^{(n)} | b_i) P(b_i).$$

At this point, one may average over all possible sequences of  $L$  information bits  $\mathbf{b}$ , thus obtaining

$$\hat{b}_i = \arg \max_{b_i=0,1} \sum_{\mathbf{b}: b_i} p(\mathcal{L}_{\text{ch}}^{(1)}, \dots, \mathcal{L}_{\text{ch}}^{(n)} | \mathbf{b}) P(\mathbf{b}) \quad (5)$$

where the notation  $\sum_{\mathbf{b}: b_i}$  denotes the sum over all sequences  $\mathbf{b}$  with  $b_i$  in the  $i$ th position. From (5), by using the total probability theorem, one obtains:

$$\begin{aligned} \hat{b}_i &= \arg \max_{b_i=0,1} \sum_{\mathbf{b}: b_i} p(\mathcal{L}_{\text{ch}}^{(1)}, \dots, \mathcal{L}_{\text{ch}}^{(n)} | \mathbf{b}) P(\mathbf{b}) \\ &= \arg \max_{b_i=0,1} \sum_{\mathbf{b}: b_i} \sum_{\mathbf{x}^{(1)}, \dots, \mathbf{x}^{(n)}} p(\mathcal{L}_{\text{ch}}^{(1)}, \dots, \mathcal{L}_{\text{ch}}^{(n)} | \mathbf{x}^{(1)}, \dots, \mathbf{x}^{(n)}) \\ &P(\mathbf{x}^{(1)}, \dots, \mathbf{x}^{(n)} | \mathbf{b}) P(\mathbf{b}) \quad (6) \\ &= \arg \max_{b_i=0,1} \sum_{\mathbf{b}: b_i} \sum_{\mathbf{x}^{(1)}, \dots, \mathbf{x}^{(n)}} \sum_{\mathbf{s}^{(1)}, \dots, \mathbf{s}^{(n)}} p(\mathcal{L}_{\text{ch}}^{(1)}, \dots, \mathcal{L}_{\text{ch}}^{(n)} | \mathbf{s}^{(1)}, \dots, \mathbf{s}^{(n)}) \\ &P(\mathbf{s}^{(1)}, \dots, \mathbf{s}^{(n)} | \mathbf{x}^{(1)}, \dots, \mathbf{x}^{(n)}) P(\mathbf{x}^{(1)}, \dots, \mathbf{x}^{(n)} | \mathbf{b}) P(\mathbf{b}) \end{aligned}$$

where, in the last line, we have exploited the fact that the joint PDF of  $\{\mathcal{L}_{\text{ch}}^{(1)}, \dots, \mathcal{L}_{\text{ch}}^{(n)}\}$ , conditionally on  $\{\mathbf{s}^{(1)}, \dots, \mathbf{s}^{(n)}\}$ , does not depend on  $\mathbf{b}$ . The probability

$P(\mathbf{s}^{(1)}, \dots, \mathbf{s}^{(n)} | \mathbf{x}^{(1)}, \dots, \mathbf{x}^{(n)})$  is equal to one if  $\{\mathbf{s}^{(1)}, \dots, \mathbf{s}^{(n)}\}$  are the codewords associated with  $\{\mathbf{x}^{(1)}, \dots, \mathbf{x}^{(n)}\}$ , respectively, or to zero otherwise. Since the information sequences  $\{\mathbf{x}^{(1)}, \dots, \mathbf{x}^{(n)}\}$  are coded independently, it follows that:

$$P(\mathbf{s}^{(1)}, \dots, \mathbf{s}^{(n)} | \mathbf{x}^{(1)}, \dots, \mathbf{x}^{(n)}) = \prod_{i=1}^n P(\mathbf{s}^{(i)} | \mathbf{x}^{(i)}). \quad (7)$$

On the other hand, since the coded signals are sent over orthogonal block-faded channels, it holds:

$$p(\mathcal{L}_{\text{ch}}^{(1)}, \dots, \mathcal{L}_{\text{ch}}^{(n)} | \mathbf{s}^{(1)}, \dots, \mathbf{s}^{(n)}) = \prod_{i=1}^n \prod_{j=1}^N p(\mathcal{L}_{\text{ch},j}^{(i)} | s_j^{(i)}). \quad (8)$$

Finally,  $P(\mathbf{x}^{(1)}, \dots, \mathbf{x}^{(n)} | \mathbf{b})$  can be obtained from the correlation model. At this point, each addendum at the right-hand side of (6) can be evaluated and  $\hat{b}_i$  can thus be obtained.

While the above MAP strategy is exact, direct evaluation of the sums at the right-hand side of (6) is computationally intractable. In fact, the number of sums in the argument of the argmax in (6) is  $2^{L-1} \cdot (2^L)^n \cdot (2^L)^n \sim 2^{L(2n+1)}$ , where we use the symbol  $\sim$  to loosely indicate "on the order of." Moreover, each addendum of the sum in (6) is composed by three factors (neglecting the term  $P(\mathbf{b})$ ) and the complexity, in terms of summations and multiplications, is

$$\underbrace{nN}_{\text{from (8)}} \times \underbrace{n}_{\text{from (7)}} \times \underbrace{nL}_{\text{from (1)}} = n^3 LN.$$

The computational complexity of the optimal MAP fusion rule is therefore

$$\mathcal{C}_{\text{opt}} \sim 2^{L(2n+1)} \times n^3 LN. \quad (9)$$

Therefore, we propose suboptimal, but computationally feasible, strategies.

#### 3.2. Suboptimal strategies

The proposed sub-optimal strategies rely on the separation between channel decoding and fusion. The general block model of the AP is shown in Fig. 2a. While decoding is based on the channel observations (i.e., channel LLRs), fusion is based on the soft-output values generated by the channel decoder. In the following, we first describe the fusion operation, common to both (JCD and SCD) sub-optimal strategies. Then, we describe the JCD and SCD operations.

##### 3.2.1. Fusion

The MAP fusion rule reads:

$$\hat{b}_i \triangleq \arg \max_{b_i=0,1} P(b_i | \mathcal{L}_i) = \arg \max_{b_i=0,1} \sum_{\{\mathbf{x}_i\}} P(b_i | \mathcal{L}_i, \mathbf{x}_i) P(\mathbf{x}_i | \mathcal{L}_i) \quad (10)$$

<sup>3</sup> We remark that the uppercase  $P$  is used to denote the PMF of a discrete random variable, whereas the lowercase  $p$  is used to denote the probability density function (PDF) of a continuous random variable.

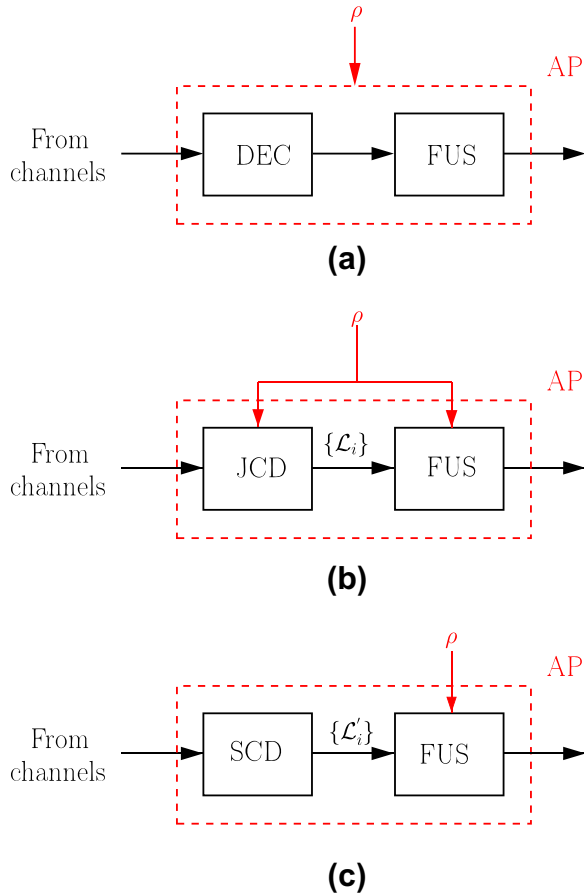


**Fig. 2.** Suboptimal approach to the CEO problem with separation of the decoding and fusion operations (case (a)). In particular, the decoding operation can be implemented by means of either JCD (case (b)) or SCD (case (c)).

where  $\mathcal{L}_i \triangleq [\mathcal{L}_i^{(1)}, \dots, \mathcal{L}_i^{(n)}]$ ,  $i = 0, \dots, L-1$ , is the vector of LLRs, relative to the information sequence  $\mathbf{x}_i$ , at the output of the  $n$  decoders,  $\mathbf{x}_i = [x_i^{(1)}, \dots, x_i^{(n)}]$  are the noisy binary observations, relative to the  $i$ th information symbol  $b_i$ , at the inputs of the sensors, and the sum in (10) is carried out over all possible  $2^n$  configurations for  $\mathbf{x}_i$ . The specific expression of  $\{\mathcal{L}_i\}$  depends on the channel decoder implementation (either JCD or SCD) and will be clearly described later.

After a few mathematical passages, the fusion rule (10) becomes

$$\hat{b}_i = \arg \max_{b_i \in \{0,1\}} \underbrace{\sum_{\{\mathbf{x}_i\}} \frac{P(\mathbf{x}_i|b_i)P(b_i)}{\sum_{b^* \in \{0,1\}} P(\mathbf{x}_i|b^*)P(b^*)}}_{\text{from the correlation model}} \underbrace{\prod_{j=1}^n P(\mathbf{x}_i^{(j)}|\mathcal{L}_i^{(j)})}_{\text{from decoder LLRs}} \quad (11)$$

where we have highlighted that each addendum of the outer sum can be expressed as a product of two terms: the first one depends only on the correlation between the observations  $\{\mathbf{x}_i^{(j)}\}$ , whereas the second one depends only on the decoder LLRs, i.e., only on the decoding scheme. Since the number of possible configurations for  $\mathbf{x}_i$  is  $2^n$  and each addendum has a complexity on the order of  $n$  products, the computational complexity, in terms of summations and multiplications, of this simplified fusion rule is

$$\mathcal{C}_{\text{sub}} \sim n2^n. \quad (12)$$

If one compares  $\mathcal{C}_{\text{sub}}$  in (12) with  $\mathcal{C}_{\text{opt}}$  in (9), it is easy to observe that the computational has been drastically reduced, since in practical applications  $n \ll L$ . Moreover, one should also consider the computational complexity needed to derive the vectors of LLRs associated

with the information sequences. However, as will be shown in Sections 3.2.2 and 3.2.3, this complexity is limited and, therefore, the computational complexity of the overall simplified fusion rule is still lower than that of the optimal MAP strategy.

The probability of decision error on a single bit can then be written as

$$P_e = P(\hat{b}_i = 0|b_i = 1)p_1 + P(\hat{b}_i = 1|b_i = 0)p_0. \quad (13)$$

The evaluation of the *average* probability of decision error, for a given value of the channel SNR, can be carried out through simulations, by averaging over a sufficiently large number of transmitted packets. However, the *asymptotic* (for very large values of the channel SNR) probability of decision error can be analytically evaluated. In this case, in fact, the decoding scheme allows to recover perfectly the effectively transmitted sequence and its limiting value (for large channel SNR) becomes

$$P_{e,\text{lim}} = p_1 \sum_{k=0}^{\lfloor \frac{n-K}{2} \rfloor - 1} \binom{n}{k} (1-\rho)^{n-k} \rho^k + p_0 \sum_{k=\lfloor \frac{n-K}{2} \rfloor}^n \binom{n}{k} (1-\rho)^k \rho^{n-k} \quad (14)$$

where  $K$  is the following function of  $\rho$  and  $p_0$ :

$$K(\rho, p_0) \triangleq \frac{\ln \frac{1-p_0}{p_0}}{\ln \frac{\rho}{1-\rho}}.$$

A formal proof of (14) is given in the Appendix A.

The limiting probability of decision error in (14) corresponds to the probability of decision error in the presence of majority fusion, as typically observed in the realm of distributed detection [14], and does not depend on the channel SNR. Therefore, the probability (14) corresponds to a floor. Moreover, the final expression (14) shows that the limiting probability of decision error *does not* depend on the particular decoding scheme under use (either JCD or SCD). However, as will be shown in Section 4, the chosen decoding scheme will affect the behavior of the probability of decision error above the limiting floor. In particular, the decoding strategy will influence the “speed” at which the floor is reached, i.e., the channel SNR at which the probability of decision error practically converges to its floor.

### 3.2.2. Joint channel decoding

In this case,  $n$  subdecoders, one per sensor, are present at the AP. Each subdecoder works on the basis of its channel LLRs and the a priori soft information obtained from the soft-output informations generated by the other subdecoders (associated with the remaining sources), properly combined taking into account the source correlation. This combining operation is carried out by a block denoted, in the following, as “COMB.” The key idea of an overall JCD iterative decoder is that of iteratively refining, by running the subdecoders, the exchanged soft information. The exchanged soft information at the input of a specific subdecoder represents an a priori “suggestion,” by the other subdecoders, on the values of the information bits at its input. Therefore, the more reliable this exchanged information, the better the performance of each subdecoder. Various activation schedules for the subdecoders can be considered and the performance of the iterative decoder depends on the chosen schedule.

In Fig. 3, two possible iterative decoding schedules are shown: (a) circular and (b) parallel. In the presence of *circular* scheduling, the subdecoders sequentially carry out their operations, exploiting the soft-output information generated by the previous subdecoders. At the very first iteration,  $\text{DEC}_1$  decodes its information bits without any a priori information and passes the soft-output values to the COMB block. At this point, a priori (input) information for  $\text{DEC}_2$  is generated only on the basis of the soft-output values output by  $\text{DEC}_1$ . After  $\text{DEC}_2$  has carried out its decoding operations, the

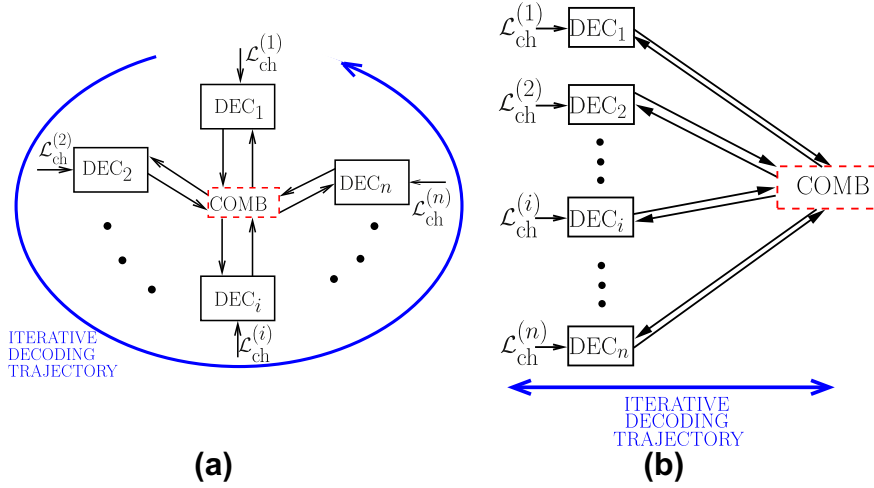


Fig. 3. JCD algorithm with (a) circular scheduling or (b) parallel scheduling.

generated soft-output values are sent to the COMB block which, in turns, generates a priori (input) information for  $\text{DEC}_3$  on the basis of the soft-output values received output by  $\text{DEC}_1$  and  $\text{DEC}_2$ . In general, during the first circular iteration the a priori (input) information for  $\text{DEC}_i$  is generated from the soft-output values output by  $\text{DEC}_{i-1}, \text{DEC}_{i-2}, \dots, \text{DEC}_1$ . From the second iteration on, the a priori information for  $\text{DEC}_i$  is generated from the most recent soft-output values output by  $\{\text{DEC}_j\}_{j \neq i}$ .

In the presence of *parallel* scheduling (illustrated in Fig. 3b), the channel subdecoders decodes carry out their decoding iterations at the same time. Therefore, at the first iteration all decoders do not use any a priori information. Once the decoders have carried out their decoding operations, the soft output values are passed to the COMB block, which acts as in the previous case with circular scheduling. From the second iteration on, each subdecoder can thus use a priori (input) information obtained from the soft values output by the other subdecoders at the previous iteration.

Regardless of the chosen scheduling, one can write that the total LLR relative to the  $i$ th observable at the input of the  $k$ th subdecoder as follows [15]:

$$\mathcal{L}_{i,\text{in}}^{(k)} = \begin{cases} \mathcal{L}_{i,\text{ch}}^{(k)} + \mathcal{L}_{i,\text{ap}}^{(k)} & i = 0, \dots, L-1 \\ \mathcal{L}_{i,\text{ch}}^{(k)} & i = L, \dots, N-1 \end{cases}$$

where the channel LLR, relative to the  $i$ th observable ( $i \in \{1, \dots, N\}$ ) from the  $k$ th node ( $k \in \{1, \dots, n\}$ ), can be expressed as in (4) and the a priori component of the LLR at the input of the  $k$ th subdecoder can be written as

$$P(\mathbf{x}_i^{(k)}) = \sum_{\mathbf{x}_i: x_i^{(k)}=0} P(\mathbf{x}_i). \quad (15)$$

Eq. (15) can be written as:

$$P(\mathbf{x}_i^{(k)}) = \sum_{\mathbf{x}_i'} P(\mathbf{x}_i^{(k)} = 0 | \mathbf{x}_i') P(\mathbf{x}_i') \quad (16)$$

where

$$\mathbf{x}_i' = \mathbf{x}_i \setminus x_i^{(k)} = (x_i^{(1)}, \dots, x_i^{(k-1)}, x_i^{(k+1)}, \dots, x_i^{(n)})^T$$

is the column vector denoting the bits at the input of the various sensors, with the exception of the  $k$ th, at time epoch  $i$ . The terms  $P(\mathbf{x}_i')$  denote the probabilities of  $n-1$  of the  $n$  sources coming from the other decoders. Assuming such  $n-1$  outputs as independent, one can write

$$P(\mathbf{x}_i) = \prod_{\substack{\ell=1 \\ \ell \neq k}}^n P(x_i^{(\ell)}).$$

The terms  $P(x_i^{(\ell)})$  can be computed from the soft output of the other component decoders and, therefore, Eq. (16) can be rewritten as

$$P(x_i^{(k)}) = \sum_{\mathbf{x}_i'} \underbrace{P(x_i^{(k)} = 0 | \mathbf{x}_i')}_{\text{a priori source correl.}} \prod_{\substack{\ell=1 \\ \ell \neq k}}^n \underbrace{\hat{P}(x_i^{(\ell)})}_{\text{from decoder } \ell}. \quad (17)$$

The interested reader is referred to [16] for an information-theoretic analysis of the capacity limits in the presence of this optimal combination rule. In [15], a simplified sub-optimal version of (17), which takes into account only the pairwise a priori probabilities, can be found. In particular, the a priori component of the LLR at the input of the  $k$ th subdecoder can be written as a weighed average (based on the correlation) of the a priori probabilities generated by the other subdecoders [15]

$$P(x_i^{(k)}) \simeq \frac{2}{n-1} \sum_{\ell=1, \ell \neq k}^n \sum_{x_i^{(\ell)=\pm 1} \text{ [from decoder } \ell]} \hat{P}(x_i^{(\ell)}) \cdot \underbrace{P(x_i^{(\ell)}, y_i^{(k)})}_{\text{[a priori source correl.]}}. \quad (18)$$

From a complexity point of view, we briefly recall a few results from [15]. Each subdecoder has a complexity  $\mathcal{C}_{\text{dec}}$ , which depends on the specific decoding algorithm under use, and is linearly dependent on the number  $N$  of coded bits:

$$\mathcal{C}_{\text{dec}} = N \mathcal{C}_{\text{dec-bit}}$$

where  $\mathcal{C}_{\text{dec-bit}}$  is the decoding complexity “per coded bit.” Moreover, at the input of each subdecoder one needs to consider a proper combination of the LLRs on the information bits output by the other  $n-1$  decoders—this operation is carried out at the COMB block. This combination has a complexity which depends linearly on the number  $L$  of information bits per sequence. In the presence of optimal LLR combination (17), the complexity required to combine  $n-1$  LLRs, relative to corresponding  $n-1$  bits at the same epoch, is on the order of  $2^n \mathcal{C}_{\text{LLR}}$ , where  $\mathcal{C}_{\text{LLR}}$  is the complexity required to combine 2 LLRs. This is due to the fact that one has to consider all the possible bit sequences of length  $n-1$ . When the sub-optimal pairwise combination (18) is considered, we can assume that the complexity required to combine  $n-1$  LLRs, relative to corresponding  $n-1$  bits at the same epoch, is on the order of  $n \mathcal{C}_{\text{LLR}}$ . Therefore, denoting the number of (circular or parallel) iterations as  $n_{\text{it}}^{\text{ext}}$ , the

overall complexity of the JCD algorithm, for the two considered combinations ((17) or (18)), can be written, regardless of the chosen scheduling, as

$$\mathcal{C}_{\text{JCD}}^{\text{opt}} \sim n_{\text{it}}^{\text{ext}} n (N \mathcal{C}_{\text{dec-bit}} + 2^n L \mathcal{C}_{\text{LLR}}) \quad (19)$$

$$\mathcal{C}_{\text{JCD}}^{\text{sub}} \sim n_{\text{it}}^{\text{ext}} n (N \mathcal{C}_{\text{dec-bit}} + n L \mathcal{C}_{\text{LLR}}). \quad (20)$$

In general, one can write

$$\mathcal{C}_{\text{JCD}} = \mathcal{C}_{\text{JCD-dec}} + \mathcal{C}_{\text{JCD-LLR}}$$

where  $\mathcal{C}_{\text{JCD-dec}} = n_{\text{it}}^{\text{ext}} n N \mathcal{C}_{\text{dec-bit}}$  is the complexity associated to decoding and is the same for the two considered combination rules.  $\mathcal{C}_{\text{JCD-LLR}}$  is the complexity associated to LLR combination, and it turns out that

$$\mathcal{C}_{\text{JCD-LLR}}^{\text{opt}} = \frac{2^n}{n} \mathcal{C}_{\text{JCD-LLR}}^{\text{sub}}.$$

Therefore, for increasing values of the number  $n$  of sources, the optimal combination rule may become unfeasible (if  $\mathcal{C}_{\text{LLR}}$  is high) and, therefore, one may have to resort to the sub-optimal pairwise combination rule. However, in Section 4 it will be shown that the performance degradation incurred by sub-optimal combination is limited.

### 3.2.3. Separate channel decoding

In order to reduce the computational complexity of the decoder, JCD, which uses the source correlation, can be replaced by SCD, which prescind from source correlation. In this case, each subdecoder separately decodes its information bits by relying only on its own channel LLRs. In other words, the input LLRs are

$$\mathcal{L}_{i,\text{in}}^{(k)} = \mathcal{L}_{i,\text{ch}}^{(k)} \quad i = 0, \dots, N-1; \quad k = 1, \dots, n.$$

Obviously, since the source correlation is not exploited, no a priori information can be derived for the subdecoders. In other words, in the presence of SCD “one-shot” per sensor decoding is considered. We remark that the fusion rule after SCD is the same derived in Sub-Section 3.2.1 and given by (11).

The computational complexity of the SCD algorithm can be straightforwardly obtained from (20) by noting that the second term at the right-hand side is not present (no LLR combination is performed) and  $n_{\text{it}}^{\text{ext}} = 1$  (no iteration is performed). Therefore, one obtains:

$$\mathcal{C}_{\text{SCD}} = \mathcal{C}_{\text{SCD-dec}} = n N \mathcal{C}_{\text{dec-bit}}$$

with a speed-up, with respect to the JCD case, approximately on the order of  $O(n_{\text{it}}^{\text{ext}})$  (assuming that LLR combination is much less computationally intense of per node decoding).

## 4. Numerical results

We now present numerical results for the proposed scenario, by means of a custom simulator written in C. In particular, each of the source sequences is encoded using a regular (3,6) low-density parity-check (LDPC) code, as in [15]. The considered LDPC code has a rate equal to  $1/2$  and  $L = 1000$ . Each component LDPC subdecoder at the AP uses a classical sum-product algorithm with a maximum number  $n_{\text{it}}^{\text{int-max}} = 50$  of internal iterations. In the presence of JCD, the number  $n_{\text{it}}^{\text{ext}}$  of external iterations between the subdecoders is fixed to 20. Finally,  $\rho$  is set<sup>4</sup> to 0.95. In most of the results presented in the remainder of this section, we will consider a binary phenomenon with equally likely statuses, i.e.,  $p_0 = p_1 = 1/2$ . However, at the end of the section we will also investigate the performance in the

case with  $p_1 = 1/10$  (i.e., rare phenomenon). For a given SNR, the results are averaged over different independent runs until at least 200 received packets or  $10^4$  received bits are erroneous. These values have been chosen in order to guarantee a 95% confidence interval. Finally, in order to bound the simulation duration, the maximum number of transmitted bits is set, for each SNR value, to  $10^9$ .

### 4.1. Partial performance analysis: decoding

We first analyze the performance of the decoding strategies presented in Sections 3.2.2 and 3.2.3, in order to highlight (i) the impact of the scheduling strategy and (ii), in the presence of SCD, the relative loss with respect to JCD schemes. The average bit error rate (BER) and the outage probability (denoted as  $P_o$ ) are the considered performance indicators. The average BER is evaluated by averaging over all  $n$  data flows and all fading generations. Concerning the outage probability, an outage event occurs when at least one bit in at least one of the  $n$  packets from the sources to the AP is in error. The outage probability is thus evaluated as the arithmetic average of the numbers of outage events over all fading generations.

In Fig. 4, the performance of JCD schemes with circular and parallel scheduling, is investigated considering various values of the number of sensors  $n$ . In Figs. 4a and 4c, the BER is shown, as a function of the SNR, in the presence of pairwise and optimal source information combination, respectively. In all cases, as expected, when the number of sources increases, the BER reduces, owing to a diversity effect. In fact, since there is a larger number of communication links, the high BER at the output of a strongly faded link can be partially lowered thanks to the reliable a priori information coming from the soft-output subdecoders associated with the other sources which experience less faded links. In the case of both pairwise and optimal source information combination, it can be observed that circular scheduling and parallel scheduling have roughly the same performance. Therefore, one may conclude that scheduling in source information combination has a minor impact.

In Figs. 4b and 4d, the outage probability is shown, as a function of the SNR, in the presence of pairwise and optimal source combination, respectively. Considerations similar to those carried out for the BER performance still hold. In this case, however, a significant difference can be highlighted with respect to the performance in terms of BER. In fact, the outage probability increases when the number of sources  $n$  increases (e.g., from 2 to 4). This is due to the fact that when the number of sources and, consequently, of transmitted packets increases, it is more likely that at least a bit (over all links) is in error. On the other hand, if the outage probability is the performance metric of interest, the beneficial presence of a priori information from the other (less faded) links is less noticeable than in the BER-based analysis, and the worst link dominates. Finally, one should note that the performance with pairwise or optimal source combination are very similar. This is due to the fact that, after a sufficiently large number of iterations, the decoder reliability (especially in terms of outage probability) reaches its maximum value possible.

In Fig. 5, the performance of the JCD algorithm with parallel scheduling (with pairwise and optimal source combination) is compared with that of the SCD algorithm. In Fig. 5a, the BER is shown as a function of the SNR. In this case, SCD shows a relevant performance loss. This is to be expected, since the subdecoders do not exchange any soft-information to improve their performance. More precisely, since all communication links are statistically equivalent, the performance with SCD does not depend on the number of sources  $n$ . Moreover, the use of the optimal source combination at the receiver allows to obtain a significant performance improvement (an SNR gain around 5 dB at a BER equal to  $10^{-2}$  and  $n = 2$ ) with respect to SCD. In Fig. 5b, the outage probability is

<sup>4</sup> We have performed other simulations for different values of  $\rho$  and found results similar to those presented in this paper for values of  $\rho$  higher than 0.8.

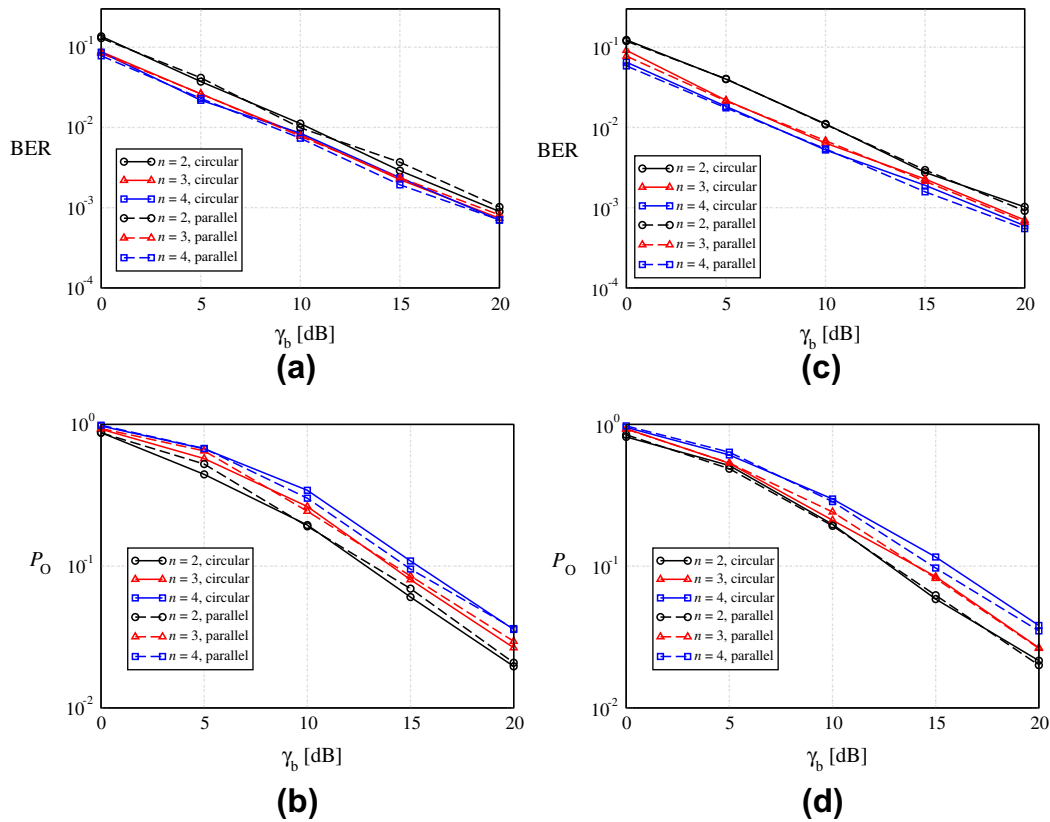


**Fig. 4.** Performance of the JCD algorithm, comparing circular and parallel scheduling: (a) BER and (b) outage probability with *pairwise* source combination and (c) BER and (d) outage probability with *optimal* source combination. Various values of  $n$  are considered and, in all cases,  $p_0 = p_1 = 1/2$ .

shown as a function of the SNR. In this case, the same considerations carried out for Fig. 4b are still valid. Therefore, the performance worsens as the number of sensors increases, and this degradation can be observed with both JCD (either with pairwise or optimal source information combination) and SCD.

At this point, one may conclude that the use of JCD is the best choice in decoding correlated sources, since SCD has a relevant performance loss and, therefore, the soft information output by a JCD is more reliable. However, as will be shown in Section 4.2, when fusion is considered this loss reduces and the decoding algorithm (either JCD or SCD) does not affect for the performance.

#### 4.2. Complete performance analysis: decoding and fusion

After analyzing the performance of the decoding block, we now evaluate the overall performance in the presence of both decoding and fusion operations. More precisely, evaluate the probability of decision error. In Fig. 6, the probability of decision error is shown, as a function of the SNR, for various values of the number of sensors  $n$ . In the decoding block, the JCD algorithm is used, with circular or parallel scheduling. The performance with pairwise source information combination in the JCD (case (a)) is compared with that associated with optimal source information combination in the JCD (case (b)).

As anticipated in Section 3.2.1, all curves reach, for large values of  $\gamma_b$ , the floor predicted by (14). In particular, since for  $p_0 = p_1 = 1/2$  the fusion rule does not improve (in terms of the floor) when  $n$  increases from an odd value (e.g., 3) to the next even value (4), no improvement is observed for the limiting performance values in Fig. 6. Comparing the results in Fig. 6 with those presented in Section 4.1, it can be concluded that the scheduling

strategy and the combination operation used in the JCD algorithm has no impact at all if information fusion is considered afterwards. In other words, this suggests that the presence of information fusion dominates over channel decoding. For the sake of completeness, in the same figure the theoretical performance limits predicted by the use of (14) is shown—they will be evaluated also in the cases considered in the following figures.

In order to validate the conjecture at the end of the previous paragraph, in Fig. 7 the probability of decision error is shown, as a function of the SNR, in a scenario with JCD and parallel scheduling (with pairwise, JCD-(2), and optimal, JCD-( $n-1$ ), source combination) is directly compared with that of a scenario with SCD. Various values of  $n$  are considered. First, all considerations about the limiting performance (in terms of probability of decision error floor) highlighted in Fig. 6 are still valid. It is interesting to observe that, while SCD has a detrimental impact on the performance at the output of the decoding algorithm (as shown in Section 4.1), this effect is highly reduced by the fusion operation. Use of optimal source information combination allows to approach the floor slightly faster for increasing values of the SNR. This allows to conclude that, when a CEO problem similar to that considered in this work is of interest, source correlation does not have to be used in the decoding algorithm, but only in the fusion operation. Therefore, a simple decoding strategy (such as SCD) can be used, thus limiting the receiver complexity without degrading its performance.

While all previous results (in both the current subsection and Section 4.1) refer to scenarios with  $p_0 = p_1 = 1/2$ , we now investigate the impact of unequal phenomenon a priori probabilities. More precisely, we consider  $p_1 = 1/10$  (rare phenomenon). In Fig. 8, the probability of decision error is shown, as a function of the SNR, for various values of the number of sensors  $n$ . In the

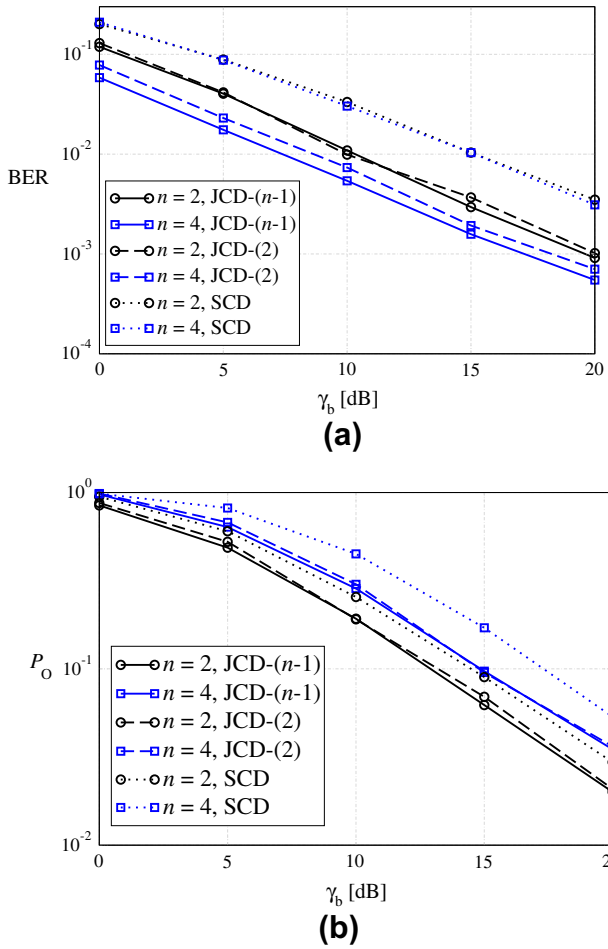


Fig. 5. Comparative performance analysis of JCD (with parallel scheduling and pairwise, JCD-(2), or optimal, JCD-(n-1), source combination) and SCD algorithms: (a) BER and (b) outage probability. Two values of  $n$  are considered (2 and 4) and, in all cases,  $p_0 = p_1 = 1/2$ .

decoding block, JCD with parallel scheduling (with pairwise, JCD-(2), and optimal, JCD-(n-1), source combination) or SCD are considered. In all cases,  $p_1 = 1/10$  ( $p_0 = 9/10$ ). The same conclusions of Fig. 7 still apply. In particular, one can observe that the perfor-

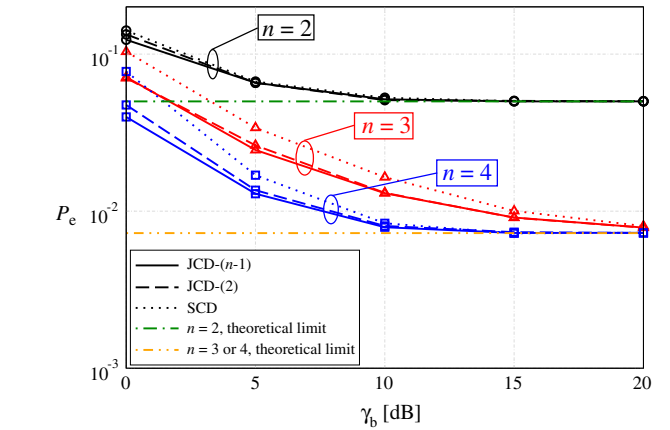
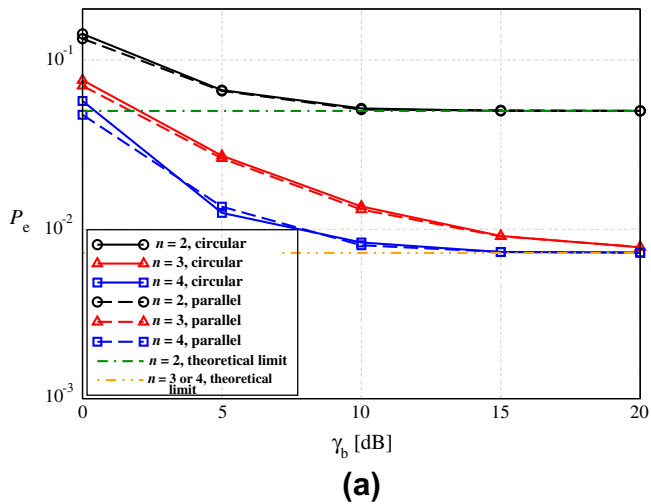


Fig. 7. Probability of decision error, as a function of the SNR, for various values of the number of sensors  $n$ . In the decoding block, JCD with parallel scheduling (with pairwise, JCD-(2), and optimal, JCD-(n-1), source combination) or SCD are considered. In all cases,  $p_0 = p_1 = 1/2$ .

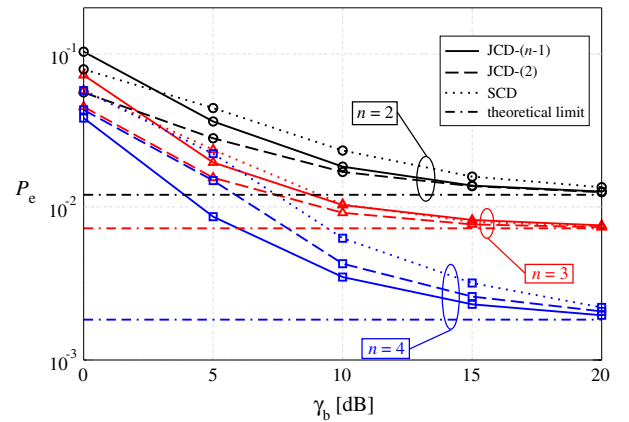


Fig. 8. Probability of decision error, as a function of the SNR, for various values of the number of sensors  $n$ . In the decoding block, JCD with parallel scheduling (with pairwise, JCD-(2), and optimal, JCD-(n-1), source combination) or SCD are considered. In all cases,  $p_1 = 1/10$  ( $p_0 = 9/10$ ).

mance loss of the SCD/fusion scheme, with respect to that of the JCD-(2)/fusion scheme is very limited. Note also that the use of

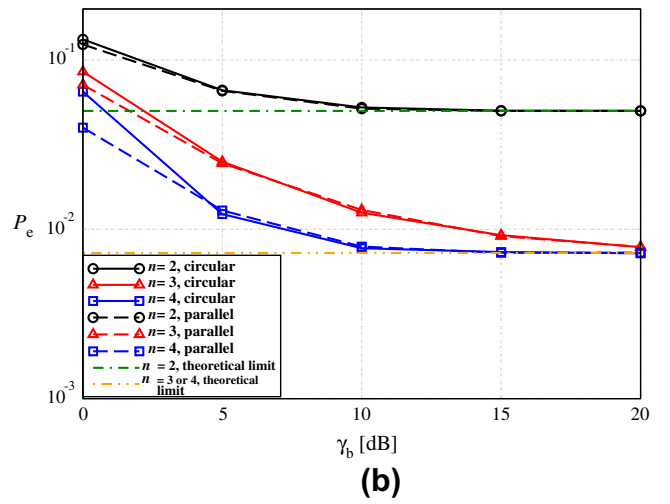


Fig. 6. Probability of decision error, as a function of the SNR, for various values of the number of sensors  $n$ . JCD is considered in the decoding block, with circular or parallel scheduling strategies. In case (a), pairwise source information combination is considered, in case (b) optimal source information combination is considered. In all cases,  $p_0 = p_1 = 1/2$ .

**Table 1**  
List of mathematical symbols used in the paper.

Symbol	Explanation
$n$	Number of sources
$L$	Information sequence length
$N$	Coded sequence length
$r$	Code rate $L/N$
$b_i$	Status (0/1) of the common binary phenomenon at the $i$ th epoch
$p_0$	Probability that $b_i = 0$
$x_i^{(k)}$	Information bit at the $i$ th epoch at the $k$ th sensor
$n_b$	Number of zeros in a given information sequence
$z_i^{(k)}$	“Correlation bit” at the $i$ th epoch at the $k$ th sensor
$\rho$	Probability that $z_i^{(k)} = 0$
$y_i^{(k)}$	Coded bit (0/1) at the $i$ th epoch at the $k$ th sensor
$\tilde{y}_i^{(k)}$	Coded bit ( $\pm 1$ ) at the $i$ th epoch at the $k$ th sensor
$E_c^{(k)}$	Energy per coded bit at the $k$ th sensor
$s_i^{(k)}$	BPSK modulated bit ( $\pm \sqrt{E_c^{(k)}}$ ) at the $i$ th epoch at the $k$ th sensor
$\alpha^{(k)}$	Fading coefficient of the $k$ th channel
$\eta_i^{(k)}$	AWGN sample at the $i$ th epoch in the $k$ th channel
$\sigma^2$	Variance of AWGN ( $N_0/2$ )
$r_i^{(k)}$	Received observable at the $i$ th epoch at the $k$ th sensor
$E_b$	Energy per information bit
$\gamma_b$	Channel SNR ( $E_b/N_0$ )
$\hat{b}_i$	Estimated status of the common phenomenon at the $i$ th epoch
$\mathcal{L}_{i,\text{ch}}^{(k)}$	Channel LLR of the $i$ th bit ( $i \in \{0, \dots, N-1\}$ ) at the $k$ th decoder
$\mathcal{L}_{i,\text{ap}}^{(k)}$	A priori LLR of the $i$ th information bit ( $i \in \{0, \dots, L-1\}$ ) at the $k$ th decoder
$\mathcal{L}_i^{(k)}$	LLR of the $i$ th information bit ( $i \in \{0, \dots, L-1\}$ ) at $k$ th decoder
$n_{\text{it}}^{\text{ext}}$	Number of external decoding iterations
$n_{\text{it}}^{\text{int-max}}$	Maximum number of internal decoding iterations

optimal source information combination (JCD- $(n-1)$ ) is beneficial only for even values of  $n$  (i.e., for odd values of  $n-1$ ). Obviously, the floor predicted by (14) is still present. Note, however, that the fusion rule now improves (in terms of the limiting performance) when  $n$  increases from an odd value (e.g., 3) to the next even value (4). As a general conclusion, the low-complexity SCD-based scheme is effective also in scenarios where a rare phenomenon is observed.

## 5. Concluding remarks

In this paper, we have analyzed a CEO scenario, where the sensors observe a noisy version of a binary sequence generated by a single source and the AP’s goal is to estimate, on the basis of the channel encoded data received by the sensors and taking into account the source correlation, this sequence. We have first derived the optimum MAP fusion rule. However, due to its unfeasible computational complexity, we have proposed two-suboptimal strategies, both based on the separation of decoding and fusion operations. According to the first strategy, source correlation is used in both decoding and fusion operations. In particular, in the decoding block JCD algorithms are considered, with: circular/parallel iterations of the a priori information between the component decoders; pairwise/optimal source information combination. According to the second strategy, source correlation is not used in the decoding block, based on SCD, but only in the fusion block. Our results have shown that the particular instance of the decoding block (SCD, JCD, circular, parallel) has a strong impact on the average BER and outage probability *before* the fusion operation. However, when the probability of error after fusion is considered as a performance indicator, the decoding strategy has a minor impact on the performance. Therefore, the use of SCD followed by fusion incurs a very limited performance loss with respect to a scheme with JCD, keeping the computational complexity very low.

## Appendix A. Derivation of the limiting probability of decision error

When the channel SNR becomes very high, the iterative decoding scheme (either JCD or SCD) allows to recover perfectly the effectively transmitted sequence, denoted as  $\mathbf{x}_i^{\text{corr}}$ . Therefore, it follows that:

$$\lim_{\gamma_b \rightarrow \infty} \left[ \prod_{j=1}^n P(x_i^{(j)} | \mathcal{L}_i^{(j)}) \right] = \begin{cases} 1 & \text{if } \mathbf{x}_i = \mathbf{x}_i^{\text{corr}} \\ 0 & \text{if } \mathbf{x}_i \neq \mathbf{x}_i^{\text{corr}} \end{cases}$$

and the fusion rule (11) becomes

$$\begin{aligned} \hat{b}_i &= \arg \max_{b_i=0,1} \frac{P(\mathbf{x}_i^{\text{corr}} | b_i) P(b_i)}{\sum_{b^*=0,1} P(\mathbf{x}_i^{\text{corr}} | b^*) P(b^*)} \\ &= \arg \max_{b_i=0,1} P(\mathbf{x}_i^{\text{corr}} | b_i) P(b_i). \end{aligned} \quad (21)$$

Denoting  $n_b = n_b(\mathbf{x}_i^{\text{corr}})$  as the number of zeros in  $\mathbf{x}_i^{\text{corr}}$ , the probability  $P(\mathbf{x}_i^{\text{corr}} | b_i)$  in (21) can be written, according to the correlation model presented in Section 2.1, as follows:

$$P(\mathbf{x}_i^{\text{corr}} | b_i) = \begin{cases} (1-\rho)^{n_b} \rho^{n-n_b} & \text{if } b_i = 0 \\ (1-\rho)^{n-n_b} \rho^{n_b} & \text{if } b_i = 1. \end{cases} \quad (22)$$

By using (22), the decision strategy (21) becomes

$$P(\mathbf{x}_i^{\text{corr}} | b_i = 0) p_0 \stackrel{b_i=0}{>} \underset{b_i=1}{<} P(\mathbf{x}_i^{\text{corr}} | b_i = 1) (1-p_0)$$

$$(1-\rho)^{n_b} \rho^{n-n_b} p_0 \stackrel{b_i=0}{>} \underset{b_i=1}{<} (1-\rho)^{n-n_b} \rho^{n_b} (1-p_0)$$

$$\left( \frac{\rho}{1-\rho} \right)^{n-2n_b} \stackrel{b_i=0}{>} \underset{b_i=1}{<} \ln \frac{1-p_0}{p_0}$$

from which one finally obtains:

$$n_b \stackrel{b_i=1}{<} \underset{b_i=0}{>} \left\lceil \frac{n - \frac{\ln \frac{1-p_0}{p_0}}{\ln \frac{\rho}{1-\rho}}}{2} \right\rceil.$$

Observing that

$$\begin{aligned} P(n_b = k | b_i = 0) &= \binom{n}{k} \rho^{n-k} (1-\rho)^k \\ P(n_b = k | b_i = 1) &= \binom{n}{k} (1-\rho)^{n-k} \rho^k \end{aligned}$$

after a few manipulations, one obtains (14).

## Appendix B. List of mathematical symbols

In Table 1, the list of mathematical symbols used in this paper is summarized.

## References

- [1] I. Akyildiz, W. Su, Y. Sankarasubramaniam, E. Cayirci, A survey on sensor networks, *IEEE Commun. Mag.* 40 (8) (2002) 102–114.
- [2] P. Gupta, P. Kumar, The capacity of wireless networks, *IEEE Trans. Inform. Theory* 46 (2) (2000) 388–404.
- [3] H.E. Gamal, On the scaling laws of dense wireless sensor networks: the data gathering channel, *IEEE Trans. Inform. Theory* 51 (3) (2005) 1229–1234.
- [4] J. Barros, S.D. Servetto, Network information flow with correlated sources, *IEEE Trans. Inform. Theory* 52 (1) (2006) 155–170.
- [5] D. Slepian, J.K. Wolf, Noiseless coding of correlated information sources, *IEEE Trans. Inform. Theory* 19 (4) (1973) 471–480.
- [6] J. Bajcsy, P. Mitran, Coding for the Slepian-Wolf problem with turbo codes, in: *Proc. IEEE Global Telecommun. Conf. (GLOBECOM)*, vol. 2, San Antonio, TX, USA, 2001, pp. 1400–1404.

- [7] Z. Xiong, A.D. Liveris, S. Cheng, Distributed source coding for sensor networks, *IEEE Signal Processing Mag.* 21 (5) (2004) 80–94.
- [8] J. Garcia-Frias, Y. Zhao, Compression of correlated binary sources using turbo codes, *IEEE Commun. Lett.* 5 (10) (2001) 417–419.
- [9] F. Daneshgaran, M. Laddomada, M. Mondin, Iterative joint channel decoding of correlated sources employing serially concatenated convolutional codes, *IEEE Trans. Inform. Theory* 51 (7) (2005) 2721–2731.
- [10] J. Muramatsu, T. Uyematsu, T. Wadayama, Low-density parity-check matrices for coding of correlated sources, *IEEE Trans. Inform. Theory* 51 (10) (2005) 3645–3654.
- [11] T. Berger, Z. Zhen, H. Viswanathan, The CEO problem, *IEEE Trans. Inform. Theory* 42 (3) (1996) 887–902.
- [12] G. Ferrari, G.M. Kouamou, C. Copioli, F. Pisani, R. Raheli, Low-complexity image processing for real-time detection of neonatal clonic seizures, in: *International Symposium on Applied Sciences in Biomedical and Communication Technologies (ISABEL 2010)*, Rome, Italy, 2010, pp. 1–5.
- [13] A. Papoulis, *Probability, Random Variables and Stochastic Processes*, McGraw-Hill, New York, NY, USA, 1991.
- [14] P.K. Varshney, *Distributed Detection and Data Fusion*, Springer-Verlag, New York, NY, USA, 1997.
- [15] A. Abrardo, G. Ferrari, M. Martalò, F. Perna, Feedback power control strategies in wireless sensor networks with joint channel decoding, *MDPI Sensors* 9 (11) (2009) 8776–8809.
- [16] G. Ferrari, M. Martalò, A. Abrardo, R. Raheli, Orthogonal multiple access coded schemes and information fusion: how many correlated sources are needed?, in: *Information Theory and Applications Workshop (ITA 2012)*, San Diego, CA, USA, 2012, pp. 311–320.